J. Inst. Eng. India Ser. C
https://doi.org/10.1007/s40032-023-00943-y

ORIGINAL CONTRIBUTION

Heat Transfer Analysis in Constructal Designed Microchannels with Perforated Micro Fins

N. Y. Godi[1] · M. O. Petinrin[2]

Received: 12 October 2022 / Accepted: 4 April 2023

Abstract This paper documents 3-D numerical optimisation of combined microchannel heat sink with solid and perforated rectangular fins. Constructal design technique is deployed to construct a geometry with reduced material substrate and the effect on the heat transfer is examined. The goal of the study is to minimise the peak temperature or maximise global thermal performance. The axial length and volume of the microchannel are fixed, while the width is allowed to morph. The microelectronic device placed at the bottom of the combined heat sink emits heat flux q'' and the heat deposited at the bottom is removed using a single-phase fluid (water) of Reynolds number Re_w in a forced convection laminar regime. The computational domain is descretised and the mathematical equations that govern the fluid flow and heat transfer are solved using the CFD code. Three unique cases were considered in this study. The influence of design parameters (channel width, external shape, and velocity of fluid applied) on the performance of the combined microchannel heat sink is discussed. The study revealed that the solid material substrates used in the manufacturing of the combined microchannel heat sink can be reduced without necessarily compromising the heat transfer at certain applied Re_w. The global thermal conductance of the combined microchannel with no perforation on fins increases by 1.1% higher than the microchannel with 1-rectangular perforation on fins and 0.8% above the heat sink with 2-rectangular perforations on fins. The numerical results validation agrees with what is in the open literature.

✉ N. Y. Godi
gdxnah001@myuct.ac.za

[1] Department of Mechanical Engineering, University of Cape Town, Private Bag X3, Rondebosch 7701, South Africa

[2] Department of Mechanical Engineering, University of Ibadan, Ibadan, Nigeria

Keywords Perforated fins · CFD · Microchannels · Constructal design optimisation · Thermal management

Abbreviations

A	Channel cross-sectional area
C	Dimensionless thermal conductance
d	Diameter
d_h	Hydraulic diameter
H	Height of heat sink
k_f	Thermal conductivity of fluid
k_s	Thermal conductivity of solid wall
MCH	Microchannel
M	Microchannel width
N	Axial length of heat sink
n	Number of channels
q''	Heat flux
Re_w	Reynolds number of water
$T_{w,L}$	Exit temperature
T_{in}	Inle temperature
T_{max}	Maximum temperature
t_1	Distance from bottom to channel
t_2	Distance from the top micro heat sink to channel
t_3	Channel to channel thickness
v_{in}	Inlet velocity
V	Volume
$\mathrm{v_{el}}$	Elemental volume
W	Width of heat sink micro channel

Greek symbols

α	Thermal diffusivity
C_p	Specific heat
μ	Viscosity
ν	Kinematic viscosity
ρ	Density

Published online: 20 April 2023

ϕ	Volume fraction of solid material
τ	Shear stress

Subscripts

in	Inlet
max	Maximum
min	Minimum
opt	Optimum
out	Outlet

Introduction

In an age of relying on electronic devices for storing and communicating information, these devices are being made progressively more powerful. The workload they carry generates heat in their operating systems; heat can be detrimental to a system and reduce its life span by damaging a component or the whole system itself if not properly dissipated. Bachr & Stephan [1] defined heat, as used in thermodynamics, as the energy that crosses the boundary of a system because of the temperature difference between the system and its surroundings. The heat transfer process is basic to most aspects of life and is frequently observed in engineering systems where it finds application and poses many challenges.

Heat sinks are recognise effective heat transfer devices which remove heat from the base to a fluid by convection. They are cost-effective and are used in managing heat dispersal in microelectronic equipment due to their success in taking away heat from surfaces [2–6]. Thermal management of electronics is important due to increasing volumetric power density and the unfriendly operating environment in which they are used. This is seen in all application fields of defense, aerospace, oil and gas, remote sensing, automotive, computer processors, semiconductors, and photonics. In addition, Bailey [7] pointed out that the inability to remove heat adequately can lead to premature device damage and even failure. He added that NASA reports indicate that 50–90% of mission failure is attributable to thermal problems.

Microelectronic devices are designed so that the heat source and the heat sink have the least resistance possible. That goal leads to continuing efforts to reduce the overall thermal resistance in the device, and conversely to increase the maximised global thermal conductance in the system [8]. Kandlikar [3] showed that thermal resistance in system devices is caused by three major sources: resistance due to conduction in the heat sink; conduction resistance between the material surface of the microchannel and the coolant; resistance arising from the increased heat of the coolant. Thermal management is improved by the application of constructal law to the heat transfer device. In order to maximize heat transfer researchers have employed constructal law to design heat sinks through their geometric configuration, giving consideration to shape, flow architecture, and structure [9, 10]. Krishna et al. [11] numerically studied the effect of waviness on heat transfer and flow characteristics in micro-wavy channels. The Re and average Nu are found to be functions of channel waviness; however, the friction factor remained unchanged at higher waviness. Elevated rates of secondary flow and recirculation appear to influence the increase of Nu with waviness.

Another way heat transfer and fluid flow of flow systems are studied is by applying computational fluid dynamics (CFD). The advancement in numerical modelling has led to the development of robust CFD codes which use the numerical algorithms developed to solve fluid flow problems. Interest in the use of CFD codes has increased in recent times due to the development of inexpensive high-performance computers and programmes that have become more user-friendly. With the CFD codes, it is now possible to design, analyse and optimise systems in fluid flow, heat transfer and similar characteristics, like chemical reactions, by digital simulation. CFD has many advantages over experimental studies, as many design variables can be simultaneously used to obtain optimal configuration and to generate quantitative information about fluid flow and heat transfer in microsystems [12–14].

In order to better understand forced convection cooling in microchannels and heat sinks, it is becoming commonplace to use a geometric optimization technique that involves identifying constraints. The concept, which is based on geometry that is either unknown or missing, calls for stating the overall objective(s) and constraint(s) of the flow system [10, 15, 16]." The success of the geometric optimisation approach is overly dependent on the constructal law as propounded by Adrian Bejan, which states, *"For a finite-size open system to persist in time (to live), it must evolve in such a way that it provides easier access to the imposed (global) currents that flow through it.*" [17]. After the work of Bejan in the twentieth century, another fundamental law of nature has been documented in the twenty-first century by Pramanick. This formidable law is called *"Law of Motive Force"*. Pramanick [18][18] states the law of motive force as*: "Every motive force is self-contradictory in its existence."* And that "opposite tendencies in a system are but conserved." The law is based on the general rule that "One or more tradeoffs happen when an effort is made to effect a change. From such tradeoffs emerge the features of organization that persist (shape, dimensions, structure, rhythm)." In addition, the word "motive force" has been used in many aspects of studies: exact sciences and non-exact sciences alike. The pioneers of thermodynamics [20, 21] also employed the word motive power, though the true nature has not been known until recently [17]. Several studies and geometric optimisation in microchannel heat sinks are based on this

law which involves searching for the missing geometry that maximises thermal conductance [20–22].” Constructal law is employed in a range of domains, for example, finding the general ranking of universities around the world, accessing the information on the global flow of knowledge [23, 24], providing vital information and optimal results in tactical operation and military warfare [25], as well as predicting optimal paths to achieve speed for men and women in swimming and athletics competitions [26–29]. The law’s use in the humanities, natural and social sciences [30–33] suggests that it is effective in increasing education, and knowledge of human life and nature, and is of universal application, as well as holding the key to the future progress of science and engineering [10, 34–42].

The parts used to extend primary surfaces are referred to as fins. Fins comprise a vast range of types, shapes and arrangements. In extended surfaces, conduction and convection are most often used for heat transfer, while radiation heat transfer is neglected [43, 44]. The cooling of electronic equipment using micro pin fins is gaining attention because of their capacity to dissipate high heat fluxes and improve the thermal management of microelectronic devices. Yeh [45] used an analytic approach to show how the dimension of circular and rectangular micro pin fins with fixed volume and heat transfer could be maximised. He observed that micro pin fins with insulated tips had the best aspect ratio with reduced fin volume. Díez et al., [46] reported the effect of roughness on micro pin fins which were truncated with changing diameter for hyperbolic, trapezoidal and concave parabolic designs. The efficiency and effectiveness of smooth pin fins, as well as temperature distribution, were accurately predicted by the approximate method of truncated power series.

This study looked at several research works carried out in the past and reviewed relevant literature. The novelty of this present study is displayed in the perforated rectangular fins. Shaeri and Yaghoub [47] perforated an array of solid fins and compared the performance. The researchers used air coolant in a forced convection laminar flow. Heat transfer rate is improved by perforating fins [48]. In this investigation, the combined microchannel with modelled micro solid fins, 1-perforation on fins and 2-perforations on fins are centrally positioned and investigated. The reduction in weight, cost and material in making the rectangular fins (combined microchannel) brings to the design an added advantage in terms of heat transfer. The combined microchannel is cooled using fluid (water), while the fins are added on top to augment heat transfer. The heat transfer is achieved by pumping water across the microchannel and by conduction which takes place in the solid material substrate and convection in the inner walls of the flow channel. The heat transfer is a conjugate, the heat removal is better than in the traditional heat sinks and the study appears to be the first research that considers heat transfer in combined microchannels of this form.

Governing Equations

The temperature at the outlet of the combined microchannel with rectangular solid and perforated fins is obtained by resolving the heat conduction and forced convection equations in the fluid domain simultaneously. The governing continuity, momentum and energy equations for the incompressible, steady state, laminar flow is

$$\frac{\partial u_i}{\partial X_i} = 0 \tag{1}$$

$$u_j \frac{\partial u_i}{\partial X_j} = -\frac{1}{\rho}\frac{\partial P}{\partial X_i} + \nu \frac{\partial^2 u_i}{\partial X_i^2} \tag{2}$$

$$u_j \frac{\partial T}{\partial X_j} = \alpha \frac{\partial^2 T}{\partial X_i \partial X_i} \tag{3}$$

However, for the solid domain, the momentum equation is reduced to

$$\overline{U} = 0 \tag{4}$$

And the energy equation for the same solid part is given as:

$$k_s \nabla^2 = 0 \tag{5}$$

Geometric Description and Boundary Conditions

A typical combined microchannel modelled with solid rectangular fins is shown in Fig. 1. The properties of a single-phase fluid, that is water, are considered to be constant when the flow is steady and laminar. The fluid flow velocities are considered to be in forced convection and the dominant mechanism for heat transfer in the cooling channels. Water of Reynolds number, Re_w flows across the entire axial length of the combined microchannel, while the fins are idly attached on top of the heat sink to augment heat transfer in the system. The combined microchannel heat sink is fabricated from aluminum material substrate with thermal conductivity of 202 W/m K that is commonly employed in heat removal from surfaces. In Fig. 1, the solid rectangular micro pin fins are modelled and placed on a rectangular microchannel block of the heat sink. The hydraulic diameter is labelled as d_h. The side and thickness of the micro pin fins are a_1 and b_1, the

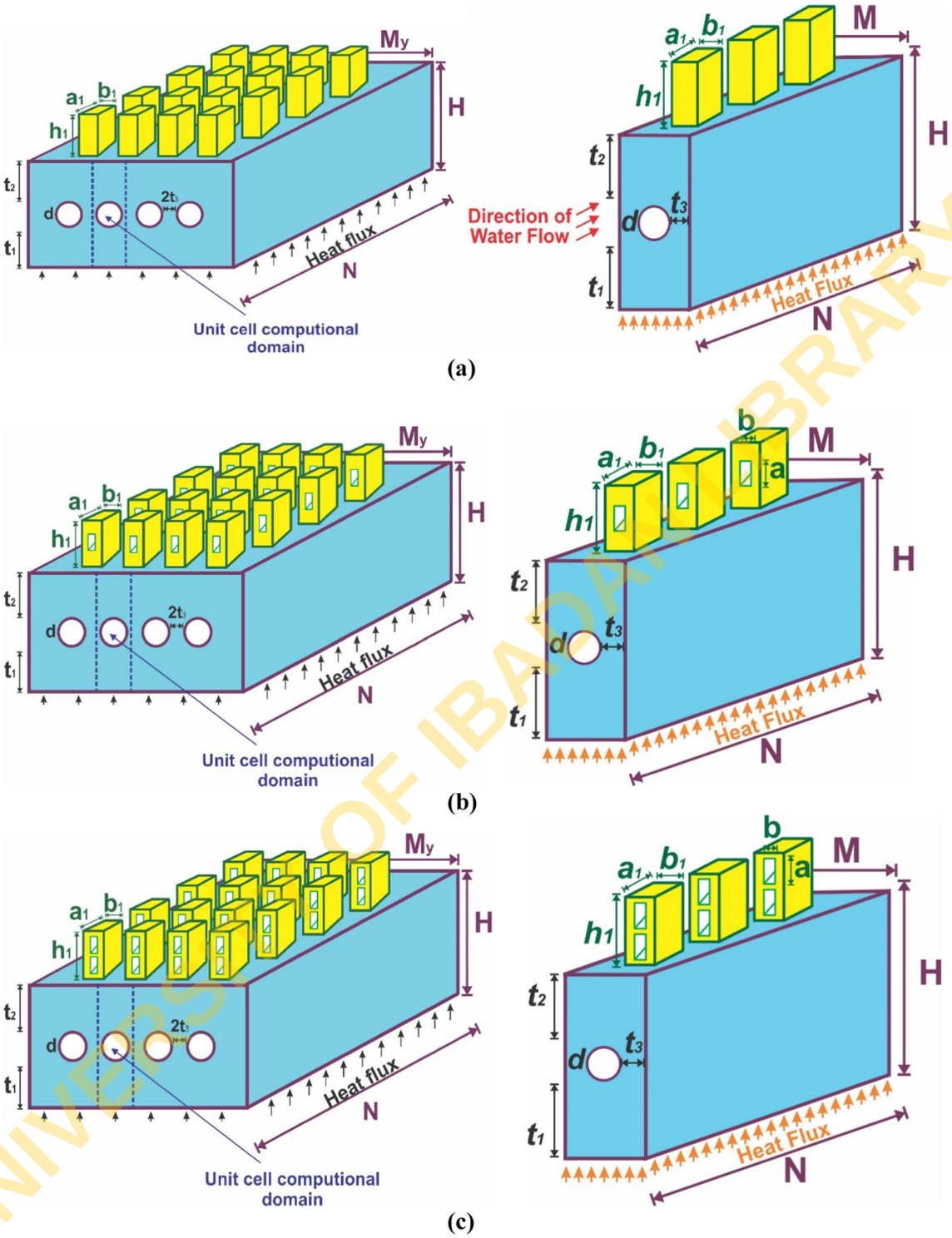

Fig. 1 shows combined microchannel heat sink with **a** no perforation on fins, **b** 1-perforation on fins and **c** 2-perforations on fins

micro pin fin height is h_1 and micro fin-to-fin spacing is S_f. In the first design (Fig. 1a), solid micro fins of length, height and width (thickness) of 40, 40 and 20 µm are modelled and placed on the rectangular block micro heat sink with a circular cooling channel, and in the second scenario, the solid fins are perforated with rectangular shape of length, height and width of 40, 12 and 6 µm, while in the third case two perforations are on each the micro pin fins with the same dimensions as in case Fig. 1b. The three-number vertical solid circular fins are centrally

mounted on the microchannels as shown in Fig. 1. The spacing between the circular fins is 50 µm and are placed at positions $f_1 = 5000\mu m, f_2 = 5050\mu m$ and $f_3 = 5100\mu m$. The unit cell rectangular block microchannel heat sink used in the simulation has an axial length N, height H, and width M. The channel-to-channel spacing is assigned t_3, the distance from the bottom of the rectangular heat sink to the lower part of the microchannel is t_1, while the distance from the top of the flow channel to the top part of the heat sink is assigned t_2. In this present investigation, the range of Reynolds numbers is between 400 and 500. The boundary conditions at the inlet and outlet of the elemental volume microchannel for fluid (water) are subjected to $u_x = u_{in}, v_y = 0, w_z = 0$, while the temperature at the entrance for fluid (water) and the air is $T = T_{in} = 25°C$ and the temperature at the wall outlet is $T = T_{w,N}$. The thermal condition applied at the bottom of the microchannel is assumed to be:

$$k_s \frac{\partial T}{\partial y} = -q'' \tag{6}$$

The heat flux continuity at the boundary between the solid body and the liquid is expressed as

$$k_s \left.\frac{\partial T}{\partial n}\right|_{wall} = k_f \left.\frac{\partial T}{\partial n}\right|_{wall} \tag{7}$$

Also, the fluid at the microchannel walls is subjected to the no-slip boundary condition.

Hence, the dimensionless maximised global thermal conductance, which is the measure of performance of the combined heat sink is given as

$$C = \frac{q'' L}{k_f \Delta T} \tag{8}$$

The elemental volume $v_{el}(NMH)$ is fixed, while t_3, t_2 and d_h are allowed to vary subject to manufacturing restrictions and the effect on the peak temperature determined. The void fraction ϕ is the ratio of the volume to the total volume of the microchannel.

The elemental volume for the microchannel is

$$v_{el} = NMH = \text{constant} \tag{9}$$

The elemental volume of the combined microchannel is

$$v_{elcom} = v_{el} + v_{elf1} + v_{elf2} + \ldots v_{elfn} = \text{constant} \tag{10}$$

where, v_{elfn} and n are the elemental volume and number of circular fins attached to the heat sink, respectively.

The elemental volume of the heat sink has a cross-sectional area of

$$A = MH \tag{11}$$

with an external aspect ratio of

$$AR = \frac{H}{M} \tag{12}$$

The void fraction or porosity of unit structure is

$$\phi = \frac{v_c}{v_{elcom}} \tag{13}$$

Manufacturing constraint for micro fins spacing is

$$S_f \geq 50\mu m \tag{14}$$

and the number of microchannels in the whole heat sink arrangement is constraint to

$$\text{number} = \frac{HM_x}{(2t_3 + b)(t_1 + t_2 + a)} \tag{15}$$

The symmetrical unit cell is inserted into the computational domain without the fins and a constant heat load, $q'' = 2.5 \times 10^6 W/m^2$ is introduced at the lower surface of the heat sink. The Reynolds number of fluid $\mathrm{Re}_w = \frac{\rho u d}{\mu}$ is applied across the entire axial length to remove the heat deposited at the bottom wall.

Figures 1a, b and c, show rectangular micro pin fins designed and placed on microchannel heat sinks shown in Figs. 1a, b and c. A circular flow channel of hydraulic diameter,d is drilled through the heat sink. The rectangular solid micro fins have sides a_1 and b_1 and height h_1, and q'' is applied on the heat sink bottom surface. The unit cell microchannel heat sinks ($v_{el} = NHM$) in Figs. 1a, b and c are chosen for simulation and optimisation based on constructal technique. The temperature at the inlet and outlet are T_{in} and T_{out} for all the configurations studied.

In Fig. 1b, the solid rectangular micro fins are perforated into rectangular shape to reduce the weight and to examine the effect on heat transfer, while in the third design double perforations of rectangular shapes are made. The sides of the perforated rectangular shapes are a and b. Three perforations on the unit cell in Fig. 1b and six perforations on the computational unit cell in Fig. 1c. The weight and volume are reduced drastically for each of the configurations and the heat transfer is a conjugate approach.

Grid Refinement and Domain Descretisation

The constructal design approach is employed to construct and geometry in the design modeler workbench of ANSYS Fluent 18.1 commercial package. The domain in the combined microchannel with solid rectangular fins has an entrance region in the channel of the micro heat sink and an exit outlet as illustrated in Fig. 1. Table 1 shows the

Table 1 The combined microchannel dimensions for the grid refinement test

N mm	d_h µm	M mm	H mm	h_1 mm	a_1 mm	b_1 mm	t_2 mm	t_3 mm
10	0.036	0.1	0.15	0.04	0.04	0.02	0.064	31.83

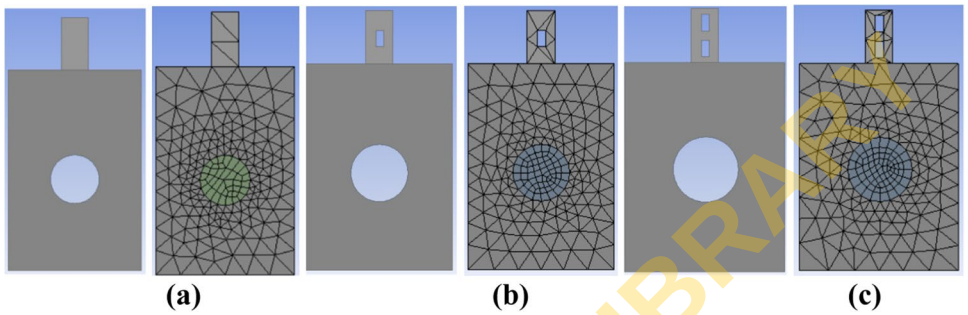

Fig. 2 3-D descretised domain of combined microchannel with solid rectangular fins

dimension of the combined microchannel with fins used in the grid refinement test. The flow domain was descretised (Fig. 2) using the hexahedral mesh Kepler [49], while in the solid material part and fins it was tetrahedral. A fine mesh setting is selected for accuracy. For low-cost computation, reduced time and energy, the mesh cells with 1 033 776 for combined microchannel with solid rectangular fins, 1 234 763 for 1-perforation on fins and 1 311 767 for 2-perforation on fins are used. Any increase in the cells beyond 1 033 776, 1 234 763 and 1 311 767, does not change the numerical results.

Computational Methodology

The descretisation of the governing equation of continuity, momentum and energy (1)–(3) is done using the finite volume code and the SIMPLE algorithm is used for the control volume cells [50]. The momentum and energy equation is computed using the second-order upwind method, and the descretised equation is solved iteratively. The computation determined the flow field by solving the continuity and momentum equations and the energy equations give the thermal field in the fluid and solid regions. A grid study is done on the mesh size until an insignificant change in temperature is obtained and the convergence solution. The monitored quantity temperature is $\gamma \leq 0.01$.

Validation

The models (combined microchannels with rectangular fins) used in this study were unable to find suitable experimental or numerical investigation in three-dimensional conditions to validate or compare with, but numerous research works that used circular flow channels are in the open literature. To validate the present numerical code, the geometry of Khan et al. [51] was modeled and numerically simulated. The

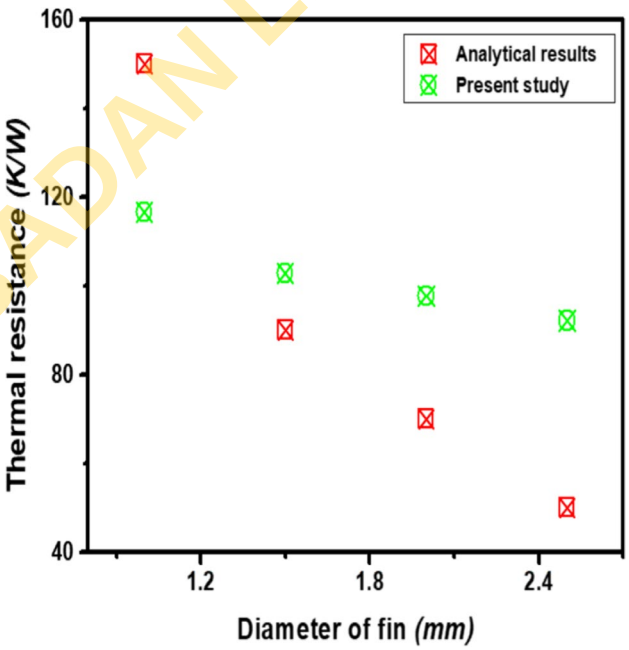

Fig. 3 CFD code validation for thermal resistance in a heat sink with fins

numerical results obtained is compared with the analytical results of Khan et al. [51]. Figure 3 shows agreement with deviations of 12.1%. The results assess the confidence of the numerical code used in this present prediction.

Numerical Results Presentation and Discussion

In this section, the results of numerical optimisation of combined microchannels with solid rectangular fins, 1- perforation on fins and 2-perforations on fins are presented and discussed. The simulation and optimisation are performed on

the microchannel and fins with a fixed total volume 0.15 to 1.7mm^3 and varying axial length 10mm. The hydraulic diameter design space for the response surface was $36.3 \leq d_h \leq 46.7$μm. The thickness of the solid structure at the base of the microchannel t_1 is 50μm, the thickness from the top of the cooling channel to the top of the rectangular block micro heat sink, $51.3 \leq t_2 \leq 63.7$μm, and the channel-to-channel thickness, t_3 is $31.8 \leq t_3 \leq 33.3$μm. The void fraction is $0.0692 \leq \phi_1 \leq 0.1009$. The objective is the maximisation of the dimensionless global thermal conductance Eq. (8).

The trend in Fig. 4 shows the existence of an optimum design hydraulic diameter that corresponds to the minimised peak temperature in the entire material substrate.

Figure 4 presents the impact of channel hydraulic diameter on T_{max} of combined microchannel with solid rectangular fins, 1-perforation on fins and 2-perforations on fins. As the channel width enlarges, T_{max} diminishes. The performance of the combined micro heat sinks is evaluated within the Reynolds number range of $450 \leq Re_w \leq 500$. The optimisation results in Fig. 4 show that at $\mathrm{Re}_w = 450$ and 500, the combined microchannel with no perforations on fins leads with the lowest peak temperature of 347.27 and 343.87 K, with an optimal d_h lying between 0.040 to 0.042-mm. It is closely followed by the heat sink with 1-perforation on fins at $\mathrm{Re}_w = 450$ with $T_{max} = 348.14$ K, before the micro heat sink with 2-perforations on fins. But when the fluid velocity increases to 500, the combined microchannel with 2-perforations on fins performed better than the micro heat sink with 1- perforation on fins with $T_{max} = 344.22$, while heat sink with 1-perforations on fins is K 344.38 K. Any increase in hydraulic diameter beyond the value that corresponds with the minimum temperature increases the peak temperature.

Similarly, Fig. 5 reveals the effect of dimensionless diameter and Re_w on the peak temperature. The combined microchannel heat sink optimised at $\frac{d_h}{N}$ located between 0.004 to 0.0042 for all the three configurations investigated. The combined microchannel with solid micro fins performed well, followed by the heat sink with 2-perforations on fins and 1-perforations on fins in that order at $\mathrm{Re}_w = 500$. Figure 4 and 5, are similar in trend and follow the same order.

The influence of the external aspect ratio of the heat sink on peak temperature is summarised in Fig. 6. The peak temperature drops as the fluid velocity increases,

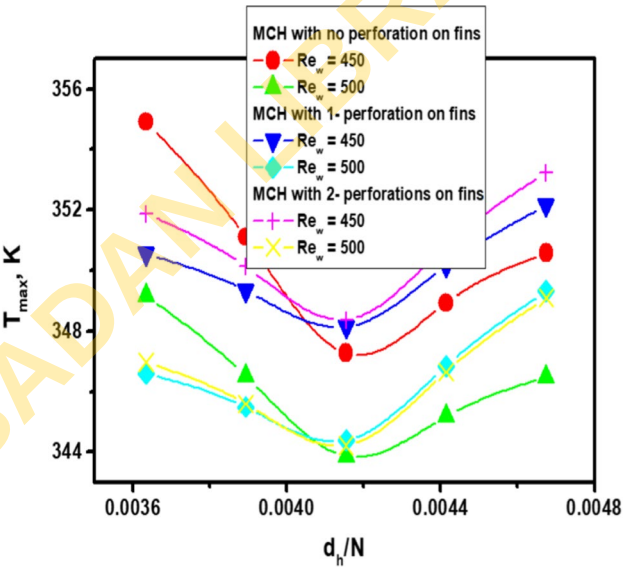

Fig. 5 Effect of dimensionless diameter on peak temperature

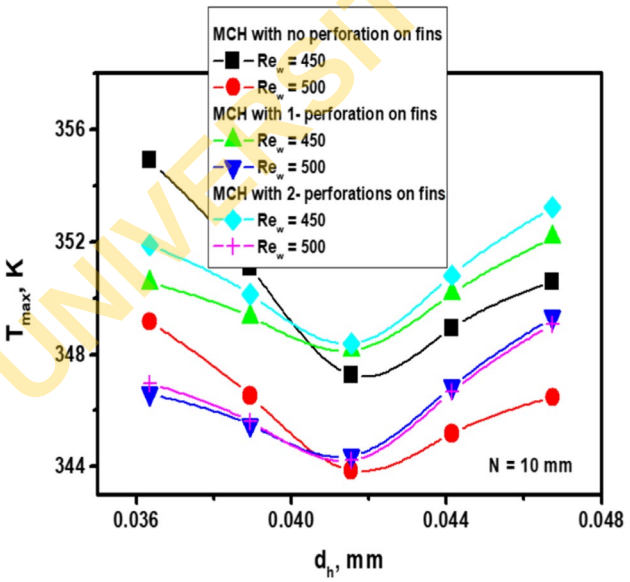

Fig. 4 Effect of channel width on peak temperature

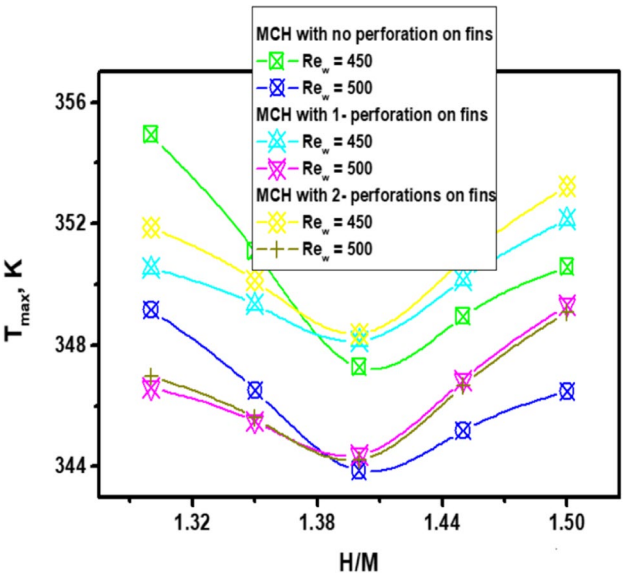

Fig. 6 Effect of eternal shape on peak temperature

as would be predicted. The peak temperature decreases until the value corresponds with the optimal design values reached. The trend shows an optimal design for the microchannel shape exit for which the peak temperature is minimised. The optimal design values for the three configurations are between 1.38 to 1.41 within the Reynolds number range of 450 to 500. The heat sinks with 1- perforation on the fins and 2-perforations on the fins have the advantage of reduced volume (weight), cost of manufacturing, and solid material. The two configurations are 9% and 27% less in solid material composition and give good cooling capabilities at an applied Reynolds number of 450 and 500.

Figure 7 depicts the effect of optimised hydraulic diameter and Reynolds number on T_{max}. The peak temperature decreases as $(d_h)_{Opt}$ increases within the Reynolds number under consideration. The optimised hydraulic diameter that produces minimum temperature in the cooling channel is in the vicinity of 0.046 mm and corresponds to 347.27, 348.14 and 348.38 K at $Re_w = 450$ for combined microchannel with rectangular solid fins (no perforation on fins), 1-perforation on fins and 2-perforations on fins. As fluid velocity increases to 500, T_{max} yields 343.87, 344.38 and 344.22 K for the heat sink with solid fins, 1-perforation on fins and 2-perforations on fins respectively. the results show that the performance of micro heat sink with 2-perforations on fins improves at a higher Reynolds number. The three configurations performed credible well and are suitable for cooling microelectronic systems. In addition, it is observed that the value of optimised hydraulic is greater than the value of channel diameter. This allows more cooling to occur within the channel at larger channel width.

Figure 8 illustrates the effect of the Reynolds number of water on the minimised temperature. As the Reynolds number increases in the range of $400 \le Re_w \le 500$, $(T_{max})_{min}$ decreases sharply by 2.6% in combined microchannel with solid rectangular fins and 1- perforation on fins, while in heat sink with 2-perforations on fins is 3%. The combined microchannel with 2-perforations on fins is preferred for cooling at $Re_w = 500$ than the heat sink with 1-perforation on fins. The trend in the results shows that the heat sink with solid rectangular fins is better, but the perforated fins are advantageous and cheaper in terms of cost and material requirement. In addition, Fig. 8 reveals that minimising the temperature increases in the global thermal conductance as seen in Fig. 9.

The effect of fluid Reynolds number on global thermal conductance C_{max} is depicted in Fig. 9. The value of C_{max} increases with an increase in Re_w. As the Re_w increases by 20%, C_{max} in the combined microchannel with solid fins increase by 16.5%, 16.4% in 1- perforation on fins and 18.6% in a heat sink with 2-perforations on fins. The combined microchannel with solid rectangular fins and no perforation has the highest heat transfer, followed by the heat sink with 2-perforations on fins and 1-perforation on fins.

The optimal geometries are correlated for global thermal conductance and Reynolds number of fluid (water) with the error level of less than 1% as seen in Eqs. (16) to (18)

$$C_{\max} = 5.51 \mathrm{Re}_w^{0.82} \text{ (MCH with no perforation on fins) } R^2 = 0.99 \quad (16)$$

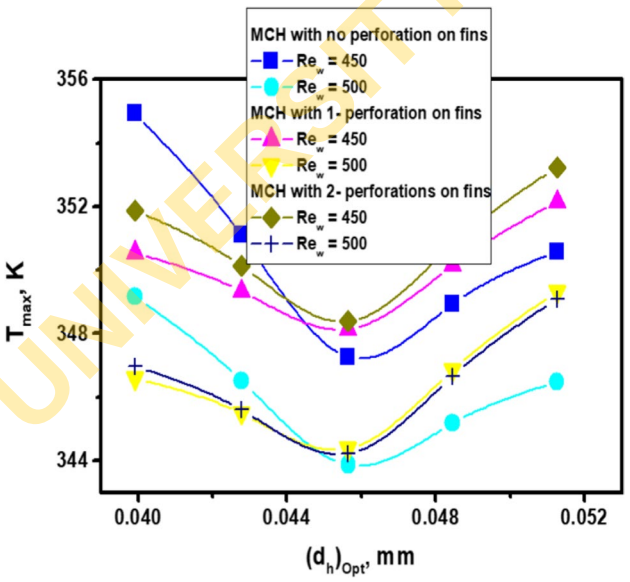

Fig. 7 Influence of optimised hydraulic diameter on peak temperature

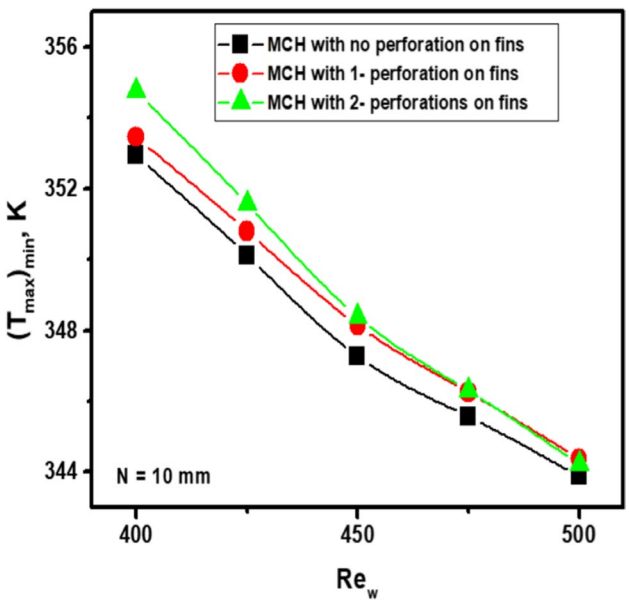

Fig. 8 Influence of fluid velocity on minimised temperature

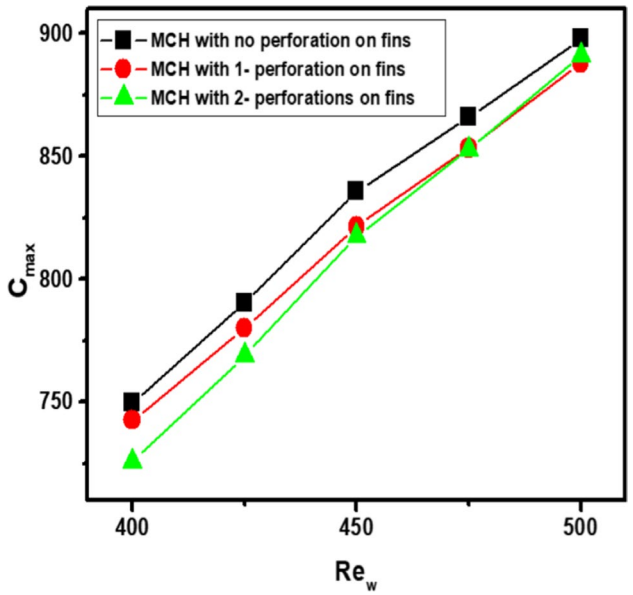

Fig. 9 Influence of fluid velocity on global thermal conductance

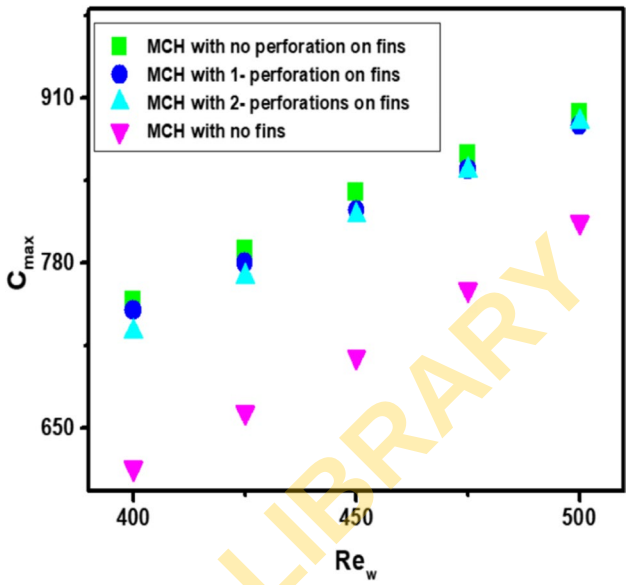

Fig. 10 Comparing global thermal conductance of combined and finless microchannels

$$C_{\max} = 5.51\mathrm{Re}_w^{0.82} \text{ (MCH with } 1- \text{ perforation on fins) } R^2 = 0.99 \quad (17)$$

$$C_{\max} = 2.78\mathrm{Re}_w^{0.93} \text{ (MCH with } 2- \text{ perforation on fins) } R^2 = 0.99 \quad (18)$$

where R^2 is the measure of how close the data is to the fitted regression, square of correlation coefficient or is called coefficient of determination on a 0 to 100% scale.

Figure 10 shows the comparison of C_{max} for combined microchannels with fins and finless microchannel heat sinks. The results reveal a directly proportional relationship between the Reynolds number and the global thermal conductance. The C_{max} in the finless microchannel heat sink increases by 23.9% as the Reynolds number of the fluid increases from 400 to 500. The heat sink without fins has the lowest heat transfer when compared with the combined microchannels with fins, as seen in Fig. 11. The relationship is correlated in Eq. (19) as

$$C_{\max} = 2.33\mathrm{Re}_w^{1.214} \text{ (MCH no fins) } R^2 = 0.99 \quad (19)$$

Temperature Gradients in Optimally Designed Geometries

Figure 11 shows the optimal design temperature contours and inner wall temperatures in combined microchannels with no perforation on fins, 1-perforation on fins and 2-perforations on fins. The red colour on the scale represents the hot zones in the combined microchannel heat sink, the greenish colour shows the medium-temperature regions, while the blue zone is the low-temperature areas. In the first case examined, for Re_w of 500 the combined microchannels with solid fins and no perforations dissipate on the outlet wall at a peak temperature of 362.8 K, but an optimised channel peak temperature of 324.2 K. In the second scenario, the combined microchannel with rectangular fins and perforated rectangular shape has $T_{max} = 366.2$ K as wall outlet temperature. The channel (fluid) peak temperature is 321.6 K at an applied $Re_w = 500$ and the same micro heat sink width M with the first case, while in the third case the peak temperature at the outlet wall is 366.1 K and the fluid or channel optimised temperature is 322 K at the same fluid velocity and combined heat sink width as in the first and second scenarios. The temperature contours and the results obtained reveal that the constructal combined microchannel designs are capable of cooling microelectronic devices and also suitable to dissipate high temperature deposited by high-density heat flux at the base wall of the combined heat sinks.

Table 2 shows the properties of the fins with solid, 1-perforation on fins and 2-perforations on fins. The decrease in the weight, volume and cost of material substrate and also the void fraction is presented. The constrcutal design technique employed in perforating the fins and compare with the unperforated fins is to minimise the volume for required heat dissipation or thermal conductance [17, 18, 48]. It is obvious that decreasing the weight by creating perforations is demonstrated in the design.

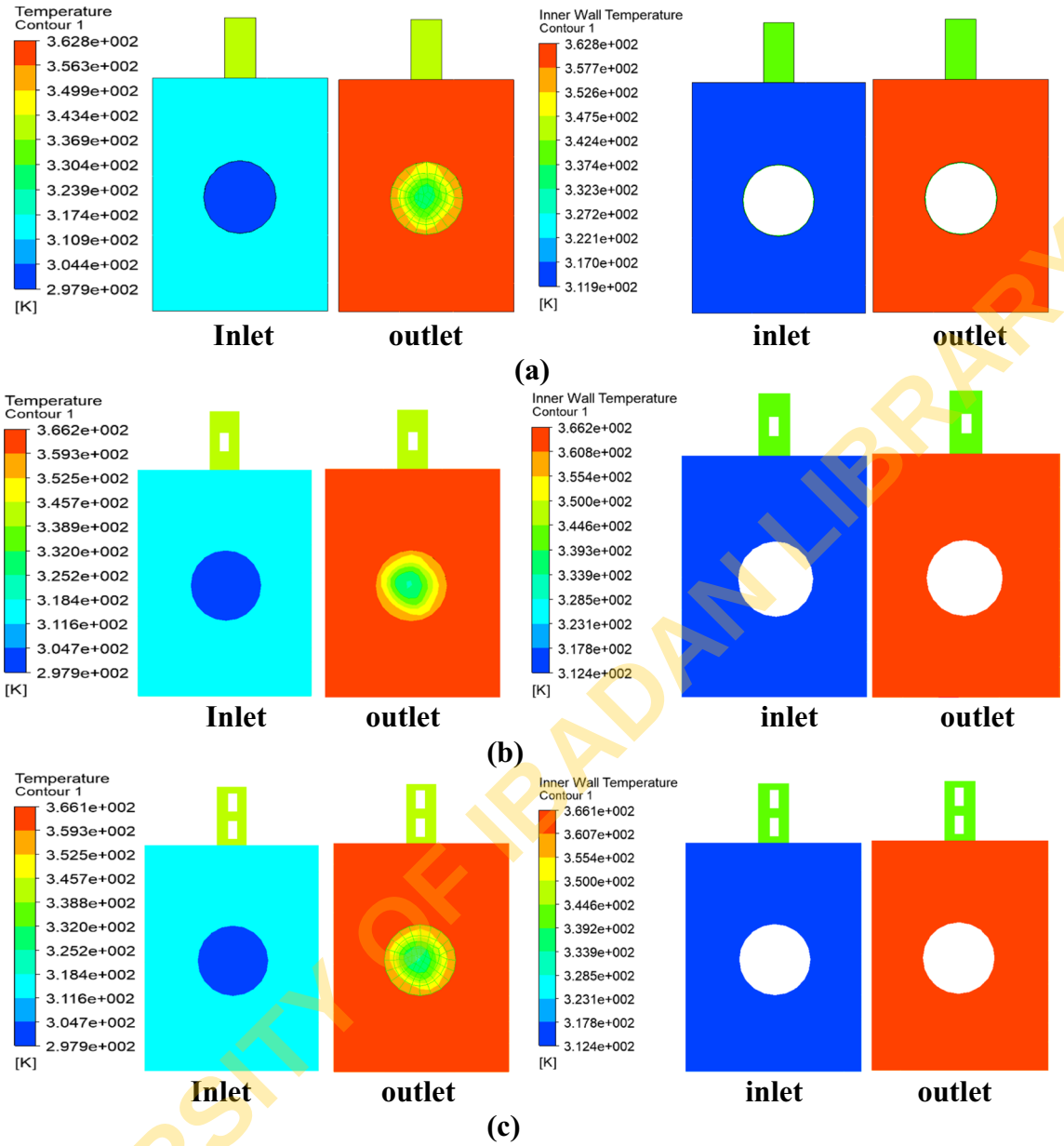

Fig. 11 Optimal temperature for microchannels with **a** no perforation on fins, **b** with 1-perforation on fins and **c** with 2-perforations on fins for $Re_w = 500$, $W = 115$ µm

Table 2 Summary of fins property

Number of fins	3 number rectangular fins		
Type of fin	Rectangular solid	Rectangular perorated	Rectangular perforated
Number of perforations	–	1	2
Volume of fins, µm^3	96,000	8640	17,280
Fin void fraction	–	0.09	0.18
% reduction in weight	–	9	18

Conclusion

In this paper, a three-dimensional numerical investigation of combined microchannels with solid rectangular fins, 1-perforation on fins and 2-perfoartions on fins under forced convection laminar fluid flow is considered. Compuation for a fluid velocity range of 400 to 500 is performed and the results show that solid fins performed better. The researchers are of the belief that if the cooling was applied to the fins, the perforated fins would have the highest heat transfer. The overall advantage of this constructal design approach is that

cost of material and manufacturing expenses and energy are saved by perforating the fins. And also the results reveal that the heat sink with 1-perforation on fins and 2-perforations on fins are 0.51 and 0.35 K above micro heat sink with solid fins. One of the significances of the study is the use of perforated fins to reduce the fin's volume and weight. The low fin weight means saving material substrate and other equipment and cost associated with heat sinks. The results have shown that perforated fins can be used to augment heat transfer and the three configurations examined are well suited for cooling integrated circuit devices.

Acknowledgements The authors appreciate the Univserity of Cape Town for the facilities used and Prof. Brandon Collier-Reed, Ass. Prof. Malebogo Ngeope, Mr. James Irlam and Engr. Tanimu Jatau, all of UCT for their support during this research.

Funding The authors have not disclosed any funding.

Declarations

Conflict of interest There are no conflicts of interest, the authors of this publication declare.

References

1. H.D. Bachr, K. Stephan, *Heat and Mass Transfer* (Springer-Verlag, Berlin Heidelberg, 1998)
2. P. Rodgers, V. Eveloy, Design challenges for high-performance heat sinks used in microelectronic equipment: Evolution and future requirements, in *Proceedings of the 5th International Conference on Thermal and Mechanical Simulation and Experiments in Microelectronics and Microsystems, EuroSimE 2004*, (2004), pp. 527–529. https://doi.org/10.1109/esime.2004.1304087
3. S.G. Kandlikar, High flux heat removal with microchannels—a roadmap of challenges and opportunities. Heat Transf. Eng. **26**, 5–14 (2005). https://doi.org/10.1080/01457630591003655
4. J. Li, G.P. Peterson, Geometric optimization of a micro heat sink with liquid flow. IEEE Trans. Components Packag. Technol. **29**, 145–154 (2006). https://doi.org/10.1109/TCAPT.2005.853170
5. I. Hassan, P. Phutthavong, M. Abdelgawad, Microchannel heat sinks: an overview of the state-of-the-art. Microscale Thermophys. Eng. **8**, 183–205 (2004). https://doi.org/10.1080/10893950490477338
6. A. Mohammed Adham, N. Mohd-Ghazali, R. Ahmad, Thermal and hydrodynamic analysis of microchannel heat sinks: a review. Renew. Sustain. Energy. Rev. **21**, 614–622 (2013). https://doi.org/10.1016/j.rser.2013.01.022
7. C. Bailey, Thermal management technologies for electronic packaging: Current capabilities and future challenges for modelling tools, in *10th Electronic Packaging Technology conference EPTC 2008*, (2008), pp. 527–532. https://doi.org/10.1109/EPTC.2008.4763487
8. V. Singh, H. Kumar, S.S. Sehgal, R. Kukreja, Effect of plenum shape on thermohydraulic performance of microchannel heat sink. J. Inst. Eng. Ser. C. (2019). https://doi.org/10.1007/s40032-019-00515-z
9. A. Bejan, S. Lorente, The constructal law and the thermodynamics of flow systems with configuration. Int. J. Heat Mass Transf. **47**, 3203–3214 (2004). https://doi.org/10.1016/j.ijheatmasstransfer.2004.02.007
10. A. Bejan, S. Lorente, The constructal law and the evolution of design in nature. Phys. Life Rev. **8**, 209–240 (2011). https://doi.org/10.1016/j.plrev.2011.05.010
11. M. Krishna, M. Deepu, S.R. Shine, Effect of relative waviness on low Re wavy microchannel flow. J. Inst. Eng. Ser. C. (2020). https://doi.org/10.1007/s40032-020-00575-6
12. Y. Jaluria, *Design and optimization of thermal system*, 2nd edn. (CRC Press, Boca Raton, 2008)
13. M.M.A. Bhutta, N. Hayat, M.H. Bashir, A.R. Khan, K.N. Ahmad, S. Khan, CFD applications in various heat exchangers design: a review. Appl. Therm. Eng. **32**, 1–12 (2012). https://doi.org/10.1016/j.applthermaleng.2011.09.001
14. J.D. Anderson, *Computational fluid dynamic: the basic with applications* (McGraw-Hill, Singapore, 1995)
15. O.T. Olakoyejo, T. Bello-Ochende, J.P. Meyer, Mathematical optimisation of laminar forced convection heat transfer through a vascularised solid with square channels. Int. J. Heat Mass Transf. **55**, 2402–2411 (2012). https://doi.org/10.1016/j.ijheatmasstransfer.2011.12.036
16. A. Bejan, S. Lorente, J. Lee, Unifying constructal theory of tree roots, canopies and forests. J. Theor. Biol. **254**, 529–540 (2008). https://doi.org/10.1016/j.jtbi.2008.06.026
17. A. Bejan, *Advanced engineering thermodynamics*, 4th edn. (Wiley, Hoboken, 2016)
18. A.K. Pramanick, *The nature of motive force* (Springer-Verlag, Berlin, 2014)
19. A.K. Pramanick, An asymptotic approach to law of motive force and constructal law. Rev. Roum. Sci. Tech.-Ser. Electrotech. Energ. **64**, 293–296 (2019)
20. T. Bello-Ochende, J.P. Meyer, F.U. Ighalo, Combined numerical optimization and constructal theory for the design of microchannel heat sinks. Numer. Heat Transf. A Appl. **58**, 882–899 (2010). https://doi.org/10.1080/10407782.2010.529036
21. T. Bello-Ochende, Maximum flow access in heat exchangers, heat generating bodies and inanimate flow systems: Constructal law and the emergence of shapes and structures in thermo-fluid mechanics. Comment on "The emergence of design in pedestrian dynamics: Locomotion, self-organization, walking paths and constructal law" by Antonio F. Miguel. Phys. Life Rev. **10**, 191–192 (2013). https://doi.org/10.1016/j.plrev.2013.03.012
22. O.T. Olakoyejo, T. Bello-Ochende, J.P. Meyer, Constructal conjugate cooling channels with internal heat generation. Int. J. Heat Mass Transf. **55**, 4385–4396 (2012). https://doi.org/10.1016/j.ijheatmasstransfer.2012.04.007
23. A. Bejan, Why university rankings do not change: education as a natural hierarchical flow architecture. Int. J. Des. Nat. Ecodynamics. **2**, 319–327 (2007). https://doi.org/10.2495/D&N-V2-N4-319-327
24. A. Bejan, Two hierarchies in science: the free flow of ideas and the academy. Int. J. Des. Nat. Ecodynamics. **4**, 386–394 (2009). https://doi.org/10.2495/DNE-V4-N4-386-394
25. G. Weinerth, The constructal analysis of warfare. Int. J. Des. Nat. Ecodynamics. **5**, 268–276 (2010). https://doi.org/10.2495/DNE-V5-N3-268-276
26. A. Bejan, J.H. Marden, Unifying constructal theory for scale effects in running, swimming and flying. J. Exp. Biol. **209**, 238–248 (2006). https://doi.org/10.1242/jeb.01974
27. J.D. Charles, A. Bejan, The evolution of speed, size and shape in modern athletics. J. Exp. Biol. **212**, 2419–2425 (2009). https://doi.org/10.1242/jeb.031161
28. A. Bejan, E.C. Jones, J.D. Charles, The evolution of speed in athletics: Why the fastest runners are black and swimmers white. Int. J. Des. Nat. Ecodynamics. **5**, 199–211 (2010). https://doi.org/10.2495/DNE-V5-N3-199-211

29. A.H. Reis, A.F. Miguel, M. Aydin, Constructal theory of flow architecture of the lungs. Med. Phys. **31**, 1135–1140 (2004). https://doi.org/10.1118/1.1705443
30. A.F. Miguel, Constructal pattern formation in stony corals, bacterial colonies and plant roots under different hydrodynamics conditions. J. Theor. Biol. **242**, 954–961 (2006). https://doi.org/10.1016/j.jtbi.2006.05.010
31. A. Nakayama, F. Kuwahara, W. Liu, A macroscopic model for countercurrent bioheat transfer in a circulatory system. J. Porous Media. **12**, 289–300 (2009). https://doi.org/10.1615/JPorMedia.v12.i4.10
32. S. Quéré, Constructal theory of plate tectonics. Int. J. Des. Nat. Ecodyn. **5**, 242–253 (2010). https://doi.org/10.2495/DNE-V5-N3-242-253
33. A.H. Reis, C. Gama, Sand size versus beachface slope—An explanation based on the Constructal Law. Geomorphology **114**, 276–283 (2010). https://doi.org/10.1016/j.geomorph.2009.07.008
34. J.P. Meyer, Constructal law in technology, thermofluid and energy systems, and in design education. Comment on "The constructal law and the evolution of design in nature" by A. Bejan and S. Lorente. Phys. Life Rev. **8**, 247–248 (2011). https://doi.org/10.1016/j.plrev.2011.07.004
35. T. Basak, The law of life: the bridge between physics and biology. Comment on "The constructal law and the evolution of design in nature" by A. Bejan and S. Lorente. Phys. Life Rev. **8**, 249–252 (2011). https://doi.org/10.1016/j.plrev.2011.07.003
36. A.F. Miguel, The physics principle of the generation of flow configuration. Comment on "The constructal law and the evolution of design in nature" by Adrian Bejan and Sylvie Lorente. Phys. Life Rev. **8**, 243–244 (2011). https://doi.org/10.1016/j.plrev.2011.07.006
37. L.A.O. Rocha, Constructal law: from law of physics to applications and conferences. Comment on "The constructal law and the evolution of design in nature" by Adrian Bejan and Sylvie Lorente. Phys. Life Rev. **8**, 245–246 (2011). https://doi.org/10.1016/j.plrev.2011.07.005
38. G. Lorenzini, C. Biserni, The constructal law: from design in nature to social dynamics and wealth as physics. Comment on "The Constructal law and the evolution of design in nature" by Professor Adrian Bejan and Professor Sylvie Lorente. Phys. Life Rev. **8**, 259–260 (2011). https://doi.org/10.1016/j.plrev.2011.08.002
39. J.A. Tuhtan, Go with the flow: connecting energy demand, hydropower, and fish using constructal theory. Comment on "The constructal law and the evolution of design in nature" by Adrian Bejan and Sylvie Lorente. Phys. Life Rev. **8**, 253–254 (2011). https://doi.org/10.1016/j.plrev.2011.07.002
40. L. Wang, Universality of design and its evolution. Comment on "The constructal law and the evolution of design in nature." Phys. Life Rev. **8**, 257–258 (2011). https://doi.org/10.1016/j.plrev.2011.08.003
41. Y. Ventikos, The importance of the constructal framework in understanding and eventually replicating structure in tissue. Comment on "The constructal law and the evolution of design in nature" by Adrian Bejan and Sylvie Lorente. Phys. Life Rev. **8**, 241–242 (2011). https://doi.org/10.1016/j.plrev.2011.07.007
42. Y.S. Kim, Design with constructal theory: steam generators, turbines and heat exchangers, Unpublished PhD. Thesis, Mechanical Engineering and Materials Science, Duke Universitya, USA, (2010)
43. J.H. Ryu, D.H. Choi, S.J. Kim, Three-dimensional numerical optimization of a manifold microchannel heat sink. Int. J. Heat Mass Transf. **46**, 1553–1562 (2003). https://doi.org/10.1016/S0017-9310(02)00443-X
44. A. Bejan, *Heat transfer* (Wiley, New Jersey, 1993)
45. R.H. Yeh, An analytical study of the optimum dimensions of rectangular fins and cylindrical pin fins. Int. J. Heat Mass Transf. **40**, 3607–3615 (1997). https://doi.org/10.1016/s0017-9310(97)00010-0
46. L.I. Díez, S. Espatolero, C. Cortés, A. Campo, Thermal analysis of rough micro-fins of variable cross-section by the power series method. Int. J. Therm. Sci. **49**, 23–35 (2010). https://doi.org/10.1016/j.ijthermalsci.2009.05.013
47. M.R. Shaeri, M. Yaghoubi, Thermal enhancement from heat sinks by using perforated fins. Energy Convers. Manag. **50**, 1264–1270 (2009). https://doi.org/10.1016/j.enconman.2009.01.021
48. B. Sahin, A. Demir, Thermal performance analysis and optimum design parameters of heat exchanger having perforated pin fins. Energy Convers. Manag. **49**, 1684–1695 (2008). https://doi.org/10.1016/j.enconman.2007.11.002
49. J. Kepler, C. Hardie, *The six-cornered snowflake* (Clarendon Press, Oxford, 1966)
50. S.V. Patankar, Numerical heat transfer and fluid flow. CRC Press (2018). https://doi.org/10.1201/9781482234213
51. W.A. Khan, J.R. Culham, M.M. Yovanovich, Performance of shrouded pin-fin heat sinks for electronic cooling. J. Thermophys. Heat Transf. **20**, 408–414 (2006). https://doi.org/10.2514/1.17713